RAA 2015 Vol. **15** No. **8**, 1154–1165 doi: 10.1088/1674–4527/15/8/005
http://www.raa-journal.org *http://www.iop.org/journals/raa*

Research in Astronomy and Astrophysics

M-giant star candidates identified in LAMOST DR 1

Jing Zhong[1], Sébastien Lépine[2,3,4], Jing Li[1], Li Chen[1], Jin-Liang Hou[1], Ming Yang[5], Guang-Wei Li[5], Yong Zhang[6] and Yong-Hui Hou[6]

[1] Key Laboratory for Research in Galaxies and Cosmology, Shanghai Astronomical Observatory, Chinese Academy of Sciences, Shanghai 200030, China; *jzhong@shao.ac.cn*
[2] Department of Physics & Astronomy, Georgia State University, 25 Park Place, Atlanta, GA 30303, USA
[3] Department of Astrophysics, Division of Physical Sciences, American Museum of Natural History, Central Park West at 79th Street, New York, NY 10024, USA
[4] City University of New York, The Graduate Center, 365 Fifth Avenue, New York, NY 10016, USA
[5] Key Laboratory of Optical Astronomy, National Astronomical Observatories, Chinese Academy of Sciences, Beijing 100012, China
[6] Nanjing Institute of Astronomical Optics & Technology, National Astronomical Observatories, Chinese Academy of Sciences, Nanjing 210042, China

Received 2015 March 31; accepted 2015 May 22

Abstract We perform a discrimination procedure with the spectral index diagram of TiO5 and CaH2+CaH3 to separate M giants from M dwarfs. Using the M giant spectra identified from LAMOST DR1 with high signal-to-noise ratio, we have successfully assembled a set of M giant templates, which show more reliable spectral features. Combining with the M dwarf/subdwarf templates in Zhong et al., we present an extended library of M-type templates which includes not only M dwarfs with a well-defined temperature and metallicity grid but also M giants with subtypes from M0 to M6. Then, the template-fitting algorithm is used to automatically identify and classify M giant stars from LAMOST DR1. The resulting catalog of M giant stars is cross-matched with 2MASS JHK_s and WISE W1/W2 infrared photometry. In addition, we calculated the heliocentric radial velocity of all M giant stars by using the cross-correlation method with the template spectrum in a zero-velocity rest frame. Using the relationship between the absolute infrared magnitude $\mathrm{M_J}$ and our classified spectroscopic subtype, we derived the spectroscopic distance of M giants with uncertainties of about 40%. A catalog of 8639 M giants is provided. As an additional result of this analysis, we also present a catalog of 101 690 M dwarfs/subdwarfs which are processed by our classification pipeline.

Key words: stars: fundamental parameters — stars: late-type — catalogs — surveys

1 INTRODUCTION

M giants are red giant branch (RGB) stars with low surface temperature ($< 4000\,\mathrm{K}$) and high luminosity (log $L/L_{\odot} \sim$ 3–4) in the late-phase of stellar evolution. Their luminous nature allows us to use these stars as good tracers to study the outer Galactic halo and distant substructures. By selecting the M giant candidates from the Two Micron All Sky Survey (2MASS), Majewski et al. (2003) mapped the first global view of the Sagittarius Dwarf Galaxy all over the sky and found that a significant fraction of M giants in the halo of the Milky Way were contributed by the Sagittarius Dwarf Galaxy; Sharma et al. (2010) identified 16 candidate stellar halo structures at high Galactic latitude, of which 6 are new. To explore the distant region of our Galaxy's outer halo, 404 M giants were identified from the UKIRT Infrared Deep Sky Survey (UKIDSS; Lawrence et al. 2007), and the kinematic analysis indicated that the M giant candidates can be used to constrain the number of Sagittarius accretion events (Bochanski et al. 2014b). Moreover, two extremely distant giants have been confirmed by spectroscopy with a distance of $\sim$ 240–270 kpc, almost beyond the virial radius of our Galaxy (Bochanski et al. 2014a).

Until recently, most M giant candidates were selected from a photometric database, and only a small fraction of them were obtained via visible/infrared spectra (Fluks et al. 1994; Danks & Dennefeld 1994; Allen & Strom 1995; Montes et al. 1999; Lançon & Wood 2000; Mann et al. 2012). In the Sloan Digital Sky Survey (SDSS; York et al. 2000), the fraction of M giants in the M-type spectroscopic sample is about 0.5%–1.0% (West et al. 2011; Covey et al. 2008), corresponding to the spectra of several hundred giants. As an alternative efficient spectroscopic survey, the LAMOST Galactic survey project observed more M giant candidates than SDSS. In the LAMOST pilot survey, Yi et al. (2014) present 58 360 M dwarf candidates and estimate the contamination from M giants to be about 4% by using the $J-H$ color criteria (Bessell & Brett 1988). Compared with the SDSS survey, the high spectral acquisition rate and high rate of observing giants indicate the great potential of the LAMOST survey program for establishing the largest spectroscopic sample of M giants for future research.

In Zhong et al. (2015, hereafter Z15), we have performed a spectral classification of all M dwarf stars in the LAMOST commissioning data. Using the template-fitting method, 2612 spectra with a relatively high signal-to-noise ratio (SNR) were positively identified as M dwarf spectra. By examining some outliers in the spectral index distribution, we found a few spectra in our sample that are more likely to be M giants instead of M dwarfs. As we pointed out in Z15, the misclassification of giants is mainly caused by the lack of giant templates in our automated classification pipeline. Although contamination by giants is not significant in the commissioning survey, it is necessary to fix this shortcoming in our pipeline since the fraction of giants largely increased in data from the pilot survey and regular survey. Our effort at assembling the M giant templates will be devoted to classifying M-type stars well, including cases of M dwarfs/subdwarfs and M giants.

In this paper, a brief description of LAMOST Data Release 1 (DR1) is given in Section 2. In Section 3, we mainly introduce our effort at establishing the M giant spectral templates, including luminosity discrimination and temperature classification. By combining the M giant templates with M dwarf templates, we use the revised classification pipeline to classify M giant stars with different subtypes in LAMOST DR1, and the analyses and results of our classification are presented in Section 4. In the last section, a brief conclusion and discussion are provided.

2 THE LAMOST DR1

The LAMOST survey is a spectroscopic survey of stars and galaxies. Based on a quasi-meridian reflecting Schmidt telescope (Cui et al. 2012) with an effective aperture of 4 m and 4000 optical fibers, the LAMOST survey has become the most ambitious spectroscopic observation program to date and will acquire over 10 million spectra of stars and galaxies in five years (Zhao et al. 2012; Liu et al. 2015). At present, the LAMOST survey has gone through its commissioning phase (2009–2011), pilot survey (2011–2012), first year (2012–2013) and second year (2013–2014) regular survey.

The LAMOST DR1 includes the pilot survey and the first year regular survey data, with a total of 2 204 860 spectra (Luo et al. 2015a). Most of these spectra are observed through the LAMOST Experiment for Galactic Understanding and Exploration (LEGUE) survey (Deng et al. 2012). For all 1 944 406 stellar spectra in DR1, the SNR values are greater than 10 in the SDSS g or r bands. A subset of about 1.1 million stellar spectra (AFGK stars) with relatively high SNR provides the stellar parameters like the effective temperature ($T_{\rm eff}$), surface gravity ($\log g$), metallicity (Fe/H) and radial velocity (RV).

The LAMOST spectra are first reduced by the LAMOST 2D pipeline over the vacuum-wavelength scale from 3800 Å to 9000 Å, which mainly includes the processes of bias subtraction, flat-field correction, skyline substraction, wavelength calibration and flux calibration (Luo et al. 2012). The extracted spectra are then passed through the 1D pipeline to classify the spectral type and calculate the RVs and redshifts.

3 M-GIANT SPECTRAL TEMPLATES

3.1 Luminosity Class

To determine the luminosity class of M type stars, specialized discrimination methods have been developed over the years which are based on colors, proper motions and spectral indices. The color discrimination method was first introduced by Bessell & Brett (1988). They show that M giants and M dwarfs are distributed around different loci in the $[J\text{-}H,\ H\text{-}K]$ color-color diagram, which are mainly caused by differences in the opacity of molecular bands of H_2O (Bessell et al. 1998). Since M giants and M dwarfs occupy distinct loci, with the group of giants having a relatively large distance and small proper motion, Lépine & Gaidos (2011) developed a robust method using reduced proper motions (H_V) to separate the two luminosity classes of M type stars. According to the comparison of M giant and M dwarf spectra, Mann et al. (2012) suggested a classification algorithm based on spectroscopic luminosity using several gravity-sensitive molecular and atomic spectral indices. In addition, Mg_2 versus $g-r$ was also used as an effective method for discrimination (Covey et al. 2008).

Since the surface gravity is totally different for giants and dwarfs, one can use spectral features as gravitational indicators to determine the luminosity class. For late-type stars, a comparison between giant and dwarf spectra with a similar effective temperature shows that at least six molecular and atomic spectral indices in the optical wavelength bands are sensitive to gravity (Mann et al. 2012), such as Na I (5868–5918 Å), Ba II/Fe I/Mn I/Ti I (6470–6530 Å), CaH2 (6814–6846 Å), CaH3 (6960–6990 Å), TiO5 (7126–7135 Å), K I (7669–7705 Å), Na I (8172–8197 Å) and Ca II (8484–8662 Å). In our work, considering the narrow ranges of wavelengths that correspond to atomic spectral indices and the possible contamination by skylines in the red region around 8000 Å, the molecular spectral indices of TiO and CaH were used to separate M giants from dwarfs in data from LAMOST DR1.

First, we used the template-fitting method (Z15) to select M-type spectra which positively present the characteristic molecular features, e.g., TiO, VO and CaH. Then the spectral indices of TiO5, CaH2 and CaH3, as defined by Reid et al. (1995) and Lépine et al. (2007), were calculated.

Figure 1 shows the diagram of spectral indices for all M type stars we identified in LAMOST DR1. Two populations are clearly distinguishable in this diagram of spectral indices. Giants with weaker CaH molecular bands are located on the upper branch, which are consistent with the giant/dwarf discrimination by Mann et al. (2012). The number of giant candidates in the upper branch is about 10 000.

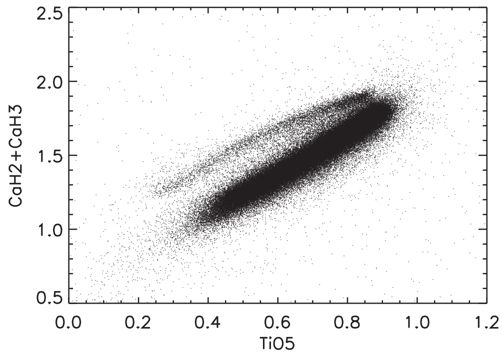

Fig. 1 The distribution of M type stars in the CaH2+CaH3 versus TiO5 diagram. Two branches in this diagram clearly indicate two populations. Because of the weaker CaH molecular bands, about 10 000 M giants are located in the upper branch. Compared with previous results (Lépine et al. 2007), the stars that are distributed in the lower branch are mainly M dwarfs/subdwarfs. A clear separation of different populations in this diagram indicates the great potential of using spectral indices to distinguish M giants from M dwarfs.

3.2 Temperature Type

As shown in Covey et al. (2007), the SDSS $r-i$ color for late-type stars has shown a good relationship with the Morgan-Keenan (MK) spectral subtypes, which span about 2 mag from M0 to M10. To provide spectral subtypes along the temperature sequence for M giants, we choose the SDSS $r-i$ color as an indicator to classify M giant subtypes.

In order to select high quality LAMOST spectra as training spectra for each spectral subtype grid, we first cross-matched the giant candidates with the SDSS DR9 photometric database. Because a large number of LAMOST stars are located in the region of the Galactic Anti-center, only about 3600 candidates have SDSS $ugriz$ photometry information. Next, to reduce the effect of extinction and to select reliable photometry, a giant candidate has to meet the following criteria:

(1) The r band extinction on Schlegel's Galactic extinction map (Schlegel et al. 1998) must be less than 0.2.
(2) The `fphotoflags` in SDSS photometry must include BRIGHT flag=0, EDGE flag=0, (BLENDED flag & NODEBLEND flag)=0, COSMIC_RAY flag=0 and SATURATED flag=0.
(3) The $g-r$ and $r-i$ color bands must be distributed on the locus of an M type star with 1.0 $< g-r <$ 1.4 mag and 0.5 $< r-i <$ 2.8 mag.

Upon applying these criteria, the training sample was cut down from $\sim$ 3600 to $\sim$ 600. Then the remaining giant candidates were confirmed by manual inspection. Giant spectra which suffer from contamination by skylines, serious reddening, low SNR or that display characteristics of a binary spectrum were excluded from the training sample. Finally, approximately 200 high quality giant spectra with good photometry in SDSS were left as the training spectra to assemble a grid representing the temperature sequence.

Table 1 lists the $r-i$ color ranges for an MK spectral subtype grid, which is mainly based on Covey et al. (2007). Since in our sample there is no giant candidate with an $r-i$ color greater than 2.0 mag, the synthetic M giant templates span the spectral subtypes from M0 to M6. For spectra with overlapping $r-i$ colors between two spectral type bins, we manually assigned the spectra by eye and made sure that the difference in spectral type was within $\pm$ 1 subtype.

Table 1 The Color Ranges of Subtype Classification

Spectral Type	$r - i$
M0.............	0.50–0.65
M1.............	0.58–0.80
M2.............	0.70–0.95
M3.............	0.90–1.10
M4.............	1.00–1.35
M5.............	1.30–1.70
M6.............	1.60–2.00

3.3 RV Correction

To correct the RV for each training spectrum, we manually used the IRAF/`rv. rvidlines` package to measure the wavelength correction to the zero-velocity rest frame. Since most atomic lines in the optical band are weak in the M giant spectrum, the near-infrared calcium (Ca II) triplet at 8498, 8542 and 8662 Å was predominantly measured as a reference wavelength. In addition, we also used the H_α (6563 Å) absorption line to calibrate early type M giants (earlier than M4), which display a significant H_α absorption feature. After measuring the wavelength correction, the training spectra were shifted toward blue or red to the zero-velocity rest frame according to their correction. The maximum RV correction in our training sample was approximately equal to $\pm$200 km s^{-1}. Then the corrected spectra were measured and shifted again. This procedure was repeated until the measured RV for each corrected training spectrum was less than 5 km s^{-1}.

3.4 Template Spectra

The wavelength corrected spectra were used to assemble the template spectra before normalizing at 8350 Å (Bochanski et al. 2007). For each spectral subtype bin, at least five training spectra were combined to create the synthetic template spectra.

Figure 2 presents the M giant template spectra from M0 to M6, which were assembled by spectra from LAMOST DR1. From top to bottom, the spectra are presented according to their temperature sequence.

To verify the reliability of our subtype classification, we calculate sets of molecular spectral indices in the synthetic template spectra as temperature indicators of giants.

Figure 3 shows the variations of different spectral indices as a function of our subtype classification. The distributions of M giants and dwarfs shown in Figure 1 are represented as green contours and blue contours in Figure 3, respectively. The indices of M giant templates are shown as red dots. From right to left, the template subtypes are from M0 to M6, which means the CaH and TiO molecular absorption bands of late-type templates are stronger than those in the early-type templates. As a comparison, we also plot the distribution of indices for M dwarf templates, which are shown as red squares. The distribution of spectral indices for giant templates shows that our template spectra are consistent with the M giant branch (upper branch in Fig. 1), and also define a reliable temperature grid.

In particular, we compare our M giant templates with Fluks' templates (Fluks et al. 1994). Figure 4 shows a comparison of the results for four spectral indices, including CaH2, CaH3, TiO5 and VO1, which were defined in Lépine et al. (2013). The templates of Fluks et al. (1994) are shown as red triangles. These intrinsic spectra were derived from 97 very bright M giant stars in the solar neighborhood, with spectral subtypes ranging from M0 to M10 and wavelengths ranging from 3800 Å to 9000 Å. Our templates are shown as green squares. The consistency of spectral indices for early type templates (M0-M5) also indicates the reliability of our classification grid. For the late type spectrum M6, there are relatively large differences between the two templates. We choose to adopt

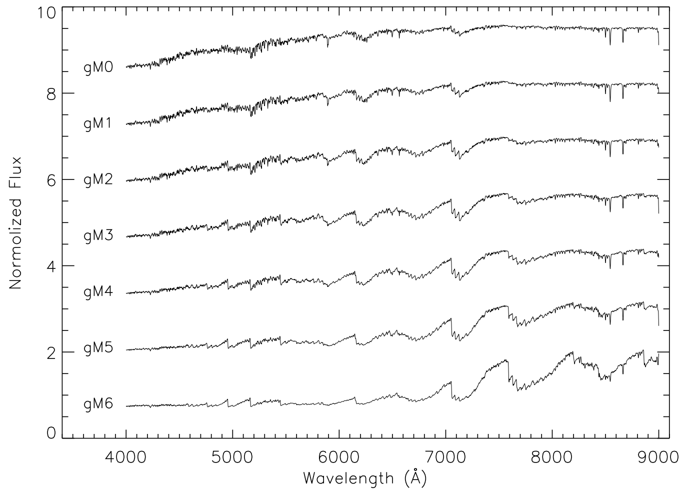

Fig. 2 The M giant templates from M0 to M6. We defined seven different giant subtypes based on the $r - i$ colors, as proposed in Table 1. Each template spectrum is assembled from at least five LAMOST spectra with high SNR which are confirmed by manual assignment. From top to bottom, the increasing strength of molecular bands, such as CaH, TiO and VO, reflect the decreasing temperature of giant spectra. The template spectra in this figure can be retrieved from the Strasbourg astronomical Data Center.

our template which comes from compiled observational spectra rather than interpolated spectra in Fluks et al. (1994).

4 SPECTRAL ANALYSES AND CLASSIFICATION RESULTS

4.1 Spectral Classification

In our previous work (Z15), a set of M dwarf templates was developed as references for automatically identifying and classifying M dwarfs in the LAMOST spectroscopic data. Our M dwarf templates were assembled from the M dwarf catalog in SDSS DR7 (West et al. 2011). Based on the spectral index method (Lépine et al. 2003, 2007), we re-classified the M dwarfs into a tentative temperature-metallicity grid with a resolution of over 18 elements in temperature (K7.0-M8.5) and a resolution of 12 elements in metallicity (dMr-usdMp). With these well defined M dwarf templates, the template-fitting method was used to determine the spectral type of LAMOST stars.

As we described in Z15, although our M dwarf templates provide a more reliable estimate of spectral classification by using the template-fitting method, because of the lack of M giant templates in our template library, a fraction of M giants are misclassified as M dwarfs. To solve this problem, we created a library of new M-type spectral templates by combining the M dwarf/subdwarf templates in Z15 with the M giant templates we described above. In the whole collection of M type templates, there are M dwarf templates with temperature from K7.0 to M8.5 and metallicity from dMr to usdMp, and M giant templates from M0 to M6. The total number of M type templates is 223.

Based on the M-type templates, we re-run our spectral classification pipeline (Z15) to automatically identify and classify M-type stars with spectra from LAMOST DR1. In order to avoid the effect of additional reddening, both template spectra and a given LAMOST spectrum were flux-normalized by a pseudo-continuum (for more details see Z15). In the classification pipeline, the template-fitting

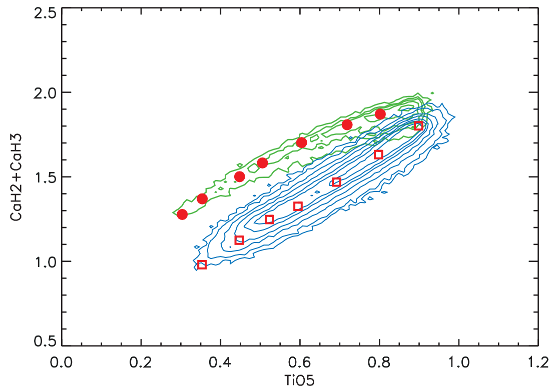

Fig. 3 To verify the reliability of the temperature sequence in our template classification, we add the spectral subtypes of giant templates into the diagram of spectral indices. From right to left, seven red dots represent the seven M giant templates from M0 to M6. For comparison, also from right to left, the seven red squares represent M dwarf templates from M0 to M6. The distributions indicate that our synthetic templates define a reliable temperature grid.

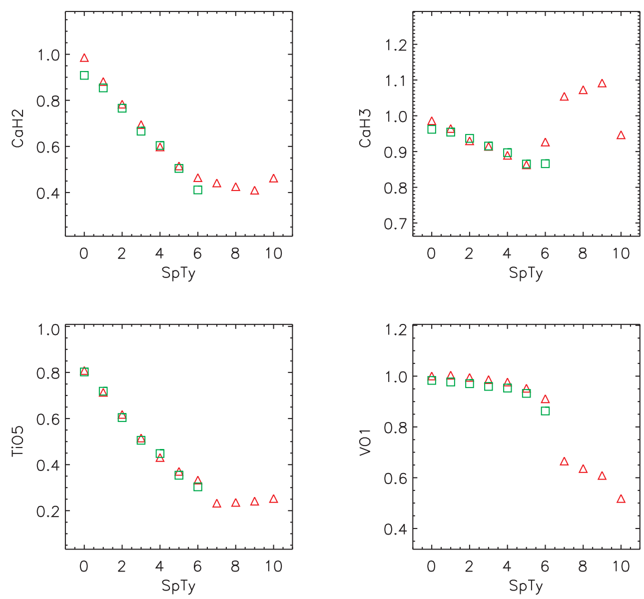

Fig. 4 Validation of the distribution of four spectral indices for the two M giant templates. The red triangles represent the spectral indices of Fluks et al. (1994), with subtypes ranging from M0 to M10. The green squares represent the spectral indices of our templates, from M0 to M6. A similar distribution shows that both M giant templates define a reliable spectral subtype grid in early type.

method was used by calculating the chi-square values between the LAMOST spectrum and each of the template spectra. Then, the template spectrum which had the minimum chi-square value was considered as the best-fit, and its spectral subtype was used to identify the corresponding LAMOST spectrum.

After applying our spectral classification pipeline to the 2 204 696 spectra from LAMOST DR1, we identified 8639 M giants and 101 690 M dwarfs/subdwarfs. The excluded spectra were marked

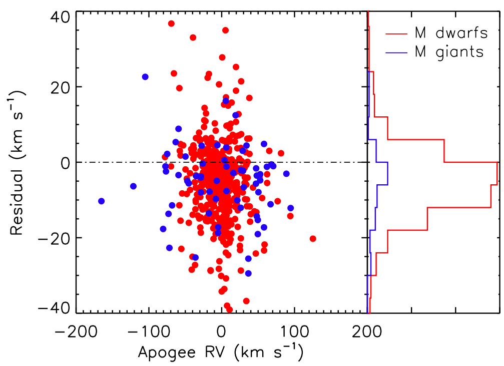

Fig. 5 Distributions of RV residuals ($RV_{\rm LAMOST}$-$RV_{\rm APOGEE}$) for all stars in both LAMOST DR1 and APOGEE data. The left plot shows the distributions of RV residuals for 59 M giants (*blue dots*) and 416 M dwarfs (*red dots*). The right plot shows the histograms of the distribution of residuals for M giants (*blue lines*) and M dwarfs (*red lines*). All the LAMOST spectra we measured have SNR greater than 10. The σ of RV residuals in our measurement is 8.4 km s^{-1} for giants and 6.9 km s^{-1} for dwarfs.

as non-M type spectra, most of which were earlier type objects like AFGK stars, and a small fraction of spectra were too noisy to be classified.

4.2 RV

To calculate the RVs of all M-type stars in our sample by using the template spectra, RV correction was applied to shift the templates into a zero-velocity rest frame as much as possible. For the M dwarf templates, the red lines of the K I doublet (7667 Å and 7701 Å) and Na I doublet (8185 Å and 8197 Å) were measured. For the M giant templates, we mainly used the Ca II triplet lines (8498, 8542, and 8662 Å) as a reference for correction (see Sect. 3 for more details). For each template spectrum, the corrected RV is less than 5 km s^{-1}, which is small enough to be considered as the zero-velocity for a low resolution spectrum.

After shifting the template spectra to the rest frame, the cross-correlation method was used to calculate the RV of each M giant spectrum in LAMOST DR1. Since the characteristic molecular bands (TiO, CaH, VO) and atomic lines (KI, NaI, CaII) of M-type stars are mainly distributed in the red part, the area where rectification was applied for normalization and cross-correlation was between 6800 Å and 8800 Å, which covers most of the characteristic wavelength range of M-type stars. Then, the best-fitting template which was determined by the classification pipeline was used to calculate the RV of LAMOST stars.

To verify the reliability of our RV measurement, we cross-matched our catalog of M-type stars with the APOGEE stellar parameter catalog in DR10. The uncertainty in RV in APOGEE data is less than 100 m s^{-1}, which can be considered as standard values. Most stars in LAMOST DR1 are located near the Galactic Anti-center, and there are about 67 giants and 575 dwarfs matched in the LAMOST DR1. We exclude common stars which have low SNR in the LAMOST spectra (SNR $<$ 10) or very strange outlier values (the total number is less than 20). Finally, we calculate the RV residuals ($RV_{\rm LAMOST}$-$RV_{\rm APOGEE}$) for 59 common giants and 416 common dwarfs. The distributions of RV residuals for M giants and M dwarfs are shown in Figure 5. The mean and standard deviation of RV errors in the Gaussian fitting are –5.0 $\pm$ 8.4 km s^{-1} for giants and –5.3 $\pm$ 6.9 km s^{-1} for dwarfs. When the SNR criterion of common stars is increased to 30, which reduces

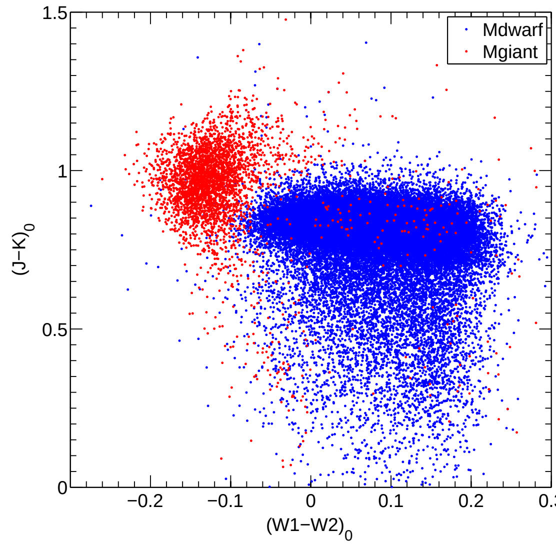

Fig. 6 The infrared color distribution of M-type stars. The red dots are M giants and the blue dots are M dwarfs, both of which were processed by our classification pipeline. As expected, the different locations of giants and dwarfs clearly show that our classification pipeline can separate the M type stars with the different luminosities well. The contamination by dwarfs in the sample of M giants is about 4.7%.

the number of giants to 39 and dwarfs to 157, we find that the mean and standard deviation of RV errors are –4.4 $\pm$ 8.1 km s^{-1} and –5.8 $\pm$ 6.5 km s^{-1}, corresponding to the M giants and M dwarfs respectively.

4.3 Estimation of the Spectroscopic Distance

To estimate the distances of M-type stars in our sample, we mainly use two independent relationships between the absolute infrared magnitude (M_J) and the spectroscopic type (SpTy). For M dwarfs, the relationship was derived by nearby M dwarfs with both spectral types and parallax measurements (Z15). Since most M dwarfs in our sample are distributed in the solar vicinity, their extinction correction is negligible in the near infrared J band. For M giants, the relationship is based on the flux calibration and absolute magnitude calculation in the 2MASS system (Covey et al. 2007). Considering that most M giants are distributed in a region that is distant from the Sun, the sample of M giants is corrected for extinction using the dust map from Schlegel et al. (1998) and the extinction law from Li et al. (2015, in preparation). This extinction law suggests that the extinction coefficients are correlated with Galactic latitude, which is believed to be more reliable in the extinction calculation, especially in low Galactic latitude. The extinction coefficients toward the Galactic Anti-center are provided in the appendix of Li et al. (2015, in preparation). Considering the magnitude and extinction uncertainties of 2MASS, the accuracy of distance values for M dwarfs/giants from the sample is estimated as 40%.

4.4 Catalog Description

In our catalog of M-type stars, the proper motions are derived by cross-matching with the PPMXL catalog (Roeser et al. 2010), and the infrared photometric information is from the 2MASS catalog

(Skrutskie et al. 2006) for the JHK_s band and the WISE catalog (Wright et al. 2010) for the W1 and W2 bands. The M giant and M dwarf candidates are listed in Table 2, and each of them has ten targets as examples. The complete catalog of M giant and M dwarf stars is provided in the electronic version of the article, including the designation in the LAMOST DR1 catalog, the celestial coordinates in epoch 2000, the proper motions and their measurement errors, the infrared photometric magnitudes, the RVs measured by our spectral template, the spectroscopic distance we estimated and the spectral subtypes which were processed by our classification pipeline.

Based on our classification results, M giants are classified along the temperature sequence, labeled as [gM0.0, gM1.0, gM2.0, gM3.0, gM4.0, gM5.0, gM6.0]. Following the classification of M dwarfs in Z15, M dwarfs are classified in the temperature-metallicity grid, which is ordered as [dMr, dMs, dMp, sdMr, sdMs, sdMp, esdMr, esdMs, esdMp, usdMr, usdMs, usdMp] in metallicity and [K7.0, K7.5, M0.0, M0.5, M1.0, M1.5, M2.0, M2.5, M3.0, M3.5, M4.0, M4.5, M5.0, M5.5, M6.0, M6.5, M7.0, M7.5, M8.0, M8.5] in temperature (for more details see Z15).

Table 2 Catalog of M-type Stars with Position, Proper Motion, Photometry, RV, Spectroscopic Distance and Estimated Subtype

Designation	RA	Dec	$\mu_\alpha \cos(\delta)$	μ_δ	J	H	K_s	W1	W2	RV	Dist	SpTy
	(°)	(°)	(mas yr^{-1})				(mag)			(km s^{-1})	(kpc)	
(1)	(2)	(3)	(4)	(5)	(6)	(7)	(8)	(9)	(10)	(11)	(12)	(13)
J040505.40+285943.6	61.27254	28.995465	4.0±5.0	–6.7±5.0	10.488	9.479	9.230	9.118	9.243	–4.3	5.16	gM0.0
J040611.64+261916.6	61.54850	26.321288	–2.7±4.4	–4.9±4.4	9.529	8.624	8.382	8.279	8.441	28.4	3.54	gM0.0
J041023.67+272143.6	62.59864	27.362117	0.0±5.2	–2.9±5.2	10.595	9.734	9.480	9.358	9.479	–19.6	5.30	gM0.0
J040325.49+293108.0	60.85623	29.518914	–0.6±5.2	–4.9±5.2	8.485	7.501	7.141	6.985	7.169	28.4	1.83	gM5.0
J040329.01+263653.4	60.87091	26.614842	–7.7±4.4	–4.9±4.4	8.661	7.676	7.316	7.197	7.330	60.4	1.95	gM5.0
J070225.22+282327.1	105.60509	28.390873	5.7±5.1	–4.7±5.1	9.909	8.928	8.656	8.535	8.615	22.1	3.60	gM4.0
J065424.57+303015.0	103.60241	30.504168	–5.9±4.1	1.4±4.1	11.229	10.433	10.197	10.126	10.246	4.0	7.71	gM0.0
J065153.21+290913.0	102.97172	29.153617	–0.7±4.9	–0.2±4.9	10.897	10.065	9.856	9.778	9.911	5.9	6.89	gM0.0
J065849.31+303318.9	104.70546	30.555272	3.7±5.1	–6.5±5.1	11.062	10.197	9.972	9.891	10.030	19.1	7.32	gM1.0
J065708.89+303001.0	104.28708	30.500294	0.3±5.0	–9.4±5.0	10.900	10.063	9.830	9.722	9.850	13.5	6.42	gM0.0
J072547.23+300200.1	111.44681	30.033388	–2.3±3.9	–12.9±3.9	15.062	14.371	14.251	14.140	14.122	–8.4	0.78	dMr0.0
J072602.89+303838.5	111.51205	30.644054	9.4±3.8	–22.1±3.8	14.648	14.013	13.732	13.682	13.586	–9.9	0.37	dMp1.5
J072724.80+305120.1	111.85334	30.855586	18.8±3.9	–12.5±3.9	14.817	14.227	14.125	13.963	13.954	–98.9	0.58	dKp7.5
J072650.49+293305.8	111.71040	29.551627	–7.1±3.8	–18.7±3.8	14.473	13.830	13.687	13.554	13.526	56.4	0.45	sdMr0.0
J072621.99+302531.5	111.59163	30.425433	0.7±3.9	–4.9±3.9	14.976	14.332	14.278	14.062	14.142	18.2	0.75	sdKr7.5
J071731.61+322753.9	109.38173	32.464975	–8.0±4.0	–29.5±4.0	12.833	12.206	11.927	11.827	11.683	–86.2	0.10	dMr4.0
J072423.08+285503.2	111.09618	28.917578	–2.9±4.0	–6.9±4.0	15.037	14.425	14.213	14.163	14.266	–212.8	0.77	dKs7.0
J072557.18+291137.1	111.48827	29.193658	9.1±3.8	–10.1±3.8	14.300	13.648	13.431	13.371	13.290	18.6	0.35	dMr1.5
J072106.54+284001.0	110.27729	28.666959	–5.4±3.9	–23.0±3.9	14.347	13.670	13.462	13.460	13.526	6.5	0.56	dKr7.5
J072037.71+292324.7	110.15716	29.390220	1.1±3.9	–3.1±3.9	14.565	13.855	13.617	13.561	13.495	8.5	0.43	dMp0.5
...	...	...	...	...	...	...	...	...	...	...	...	...

Notes: Columns (1)–(3) Designation is from the LAMOST DR1; Columns (4)–(5) $\mu_\alpha \cos(\delta)$ and μ_δ are proper motion from the PPMXL; Columns (6)–(8) J, H and K_s are 2MASS near infrared magnitude; Columns (9)–(10) W1 and W2 are WISE infrared magnitude; Column (11) RV is the radial velocity we measured from the LAMOST spectra; Column (12) Dist is the spectroscopic distance based on the M_J magnitude; Column (13) SpTy is the spectral subtype classified by our template fit pipeline. The entire table is available on *http://www.raa-journal.org/docs/Supp/ms2230_electrictables.zip*.

5 CONCLUSIONS AND DISCUSSION

We have successfully assembled a set of templates for M giants from M0 to M6 by using spectra from LAMOST DR1. After combining templates of M giants with templates of M dwarfs/subdwarfs as a new M-type spectral library, we re-run the updated classification pipeline to identify and classify M-type stars in LAMOST DR1. The 8639 M giants and the 101 690 M dwarfs/subdwarfs are cataloged.

We present information of celestial coordinates, JHK_s infrared magnitudes in 2MASS, spectral subtypes, RV and derived spectroscopic distance.

Based on our catalog of M-type stars, Li et al. (2015, in preparation) developed a new photometric method to separate M giants from M dwarfs. The WISE bands are found to be more efficient for separating M giants from dwarfs than the 2MASS bands. Figure 6 shows the distribution of our M giants and dwarfs from the catalog in the [$J - K_s$, W1–W2] color-color diagram. The two colors represent our sample of M giants (red dots) and M dwarfs (blue dots) which was processed by our spectral classification pipeline. As expected, there are significant differences between the giants and dwarfs in the infrared colors. By using the criterion of mean SNR greater than 5, the M dwarf contamination rate is about 4.7% in our giant sample and the M giant contamination rate is about 0.2% in our dwarf sample. By increasing the SNR criterion of our sample, the contamination rate will be smaller.

In Figure 6, we note that there is a tail in the giant sample, from –0.1 to 0.1 in the (W1–W2)$_0$ and 0.9 to 1.3 in the $(J - K_s)_0$. We carefully examine these tail stars and believe that they are more likely to be metal poor stars (see more details in Li et al. 2015, in preparation).

Although the different locations of M giants and M dwarfs in the sample shown in Figure 6 clearly demonstrates that our classification pipeline separates the two stellar populations more efficiently, a small number of outliers in the M giants sample are located in the M dwarf region (–0.1 $\leq$ (W1–W2)$_0 \leq 0$, $0 \leq (J - K_s)_0 \leq 0.7$). After checking these stars by their spectra, we find that there is possible contamination from late K-type dwarfs, early M dwarfs, binaries as well as some spectra with low SNR.

Acknowledgements We thank Guhathakurta Puragra and Katie Hamren for helpful information and comments. This research was supported by the "973 Program" (2014 CB845702), the Strategic Priority Research Program "The Emergence of Cosmological Structures" of the Chinese Academy of Sciences (Grant No. XDB09000000), the National Natural Science Foundation of China (NSFC, Grant No. 11173044) (PI:Hou), the Shanghai Natural Science Foundation (14ZR1446900) (PI:Zhong), the Key Project (10833005) (PI:Hou) and by the Group Innovation Project (No. 11121062).

The Guo Shou Jing Telescope (the Large Sky Area Multi-Object Fiber Spectroscopic Telescope, LAMOST) is a National Major Scientific Project built by the Chinese Academy of Sciences. Funding for the project has been provided by the National Development and Reform Commission. LAMOST is operated and managed by National Astronomical Observatories, Chinese Academy of Sciences.

References

Allen, L. E., & Strom, K. M. 1995, AJ, 109, 1379
Bessell, M. S., & Brett, J. M. 1988, PASP, 100, 1134
Bessell, M. S., Castelli, F., & Plez, B. 1998, A&A, 333, 231
Bochanski, J. J., West, A. A., Hawley, S. L., & Covey, K. R. 2007, AJ, 133, 531
Bochanski, J. J., Willman, B., Caldwell, N., et al. 2014a, ApJ, 790, L5
Bochanski, J. J., Willman, B., West, A. A., Strader, J., & Chomiuk, L. 2014b, AJ, 147, 76
Covey, K. R., Ivezić, Ž., Schlegel, D., et al. 2007, AJ, 134, 2398
Covey, K. R., Hawley, S. L., Bochanski, J. J., et al. 2008, AJ, 136, 1778
Cui, X.-Q., Zhao, Y.-H., Chu, Y.-Q., et al. 2012, RAA (Research in Astronomy and Astrophysics), 12, 1197
Danks, A. C., & Dennefeld, M. 1994, PASP, 106, 382
Deng, L.-C., Newberg, H. J., Liu, C., et al. 2012, RAA (Research in Astronomy and Astrophysics), 12, 735
Fluks, M. A., Plez, B., The, P. S., et al. 1994, A&AS, 105, 311
Lançon, A., & Wood, P. R. 2000, A&AS, 146, 217
Lawrence, A., Warren, S. J., Almaini, O., et al. 2007, MNRAS, 379, 1599

Lépine, S., Rich, R. M., & Shara, M. M. 2003, AJ, 125, 1598
Lépine, S., Rich, R. M., & Shara, M. M. 2007, ApJ, 669, 1235
Lépine, S., & Gaidos, E. 2011, AJ, 142, 138
Lépine, S., Hilton, E. J., Mann, A. W., et al. 2013, AJ, 145, 102
Liu, X. W., Zhao, G., & Hou, J. L. 2015, RAA (Research in Astronomy and Astrophysics), 15, 1089
Luo, A.-L., Zhang, H.-T., Zhao, Y.-H., et al. 2012, RAA (Research in Astronomy and Astrophysics), 12, 1243
Luo, A.-L., Zhao, Y. H., Zhao, G., et al. 2015, RAA (Research in Astronomy and Astrophysics), 15, 1095
Majewski, S. R., Skrutskie, M. F., Weinberg, M. D., & Ostheimer, J. C. 2003, ApJ, 599, 1082
Mann, A. W., Gaidos, E., Lépine, S., & Hilton, E. J. 2012, ApJ, 753, 90
Montes, D., Ramsey, L. W., & Welty, A. D. 1999, ApJS, 123, 283
Reid, I. N., Hawley, S. L., & Gizis, J. E. 1995, AJ, 110, 1838
Roeser, S., Demleitner, M., & Schilbach, E. 2010, AJ, 139, 2440
Schlegel, D. J., Finkbeiner, D. P., & Davis, M. 1998, ApJ, 500, 525
Sharma, S., Johnston, K. V., Majewski, S. R., et al. 2010, ApJ, 722, 750
Skrutskie, M. F., Cutri, R. M., Stiening, R., et al. 2006, AJ, 131, 1163
West, A. A., Morgan, D. P., Bochanski, J. J., et al. 2011, AJ, 141, 97
Wright, E. L., Eisenhardt, P. R. M., Mainzer, A. K., et al. 2010, AJ, 140, 1868
Wu, Y., Luo, A., Du, B., Zhao, Y., & Yuan, H. 2014, arXiv:1407.1980
Yi, Z., Luo, A., Song, Y., et al. 2014, AJ, 147, 33
York, D. G., Adelman, J., Anderson, Jr., J. E., et al. 2000, AJ, 120, 1579
Zhao, G., Zhao, Y.-H., Chu, Y.-Q., Jing, Y.-P., & Deng, L.-C. 2012, RAA (Research in Astronomy and Astrophysics), 12, 723
Zhong, J., Lepine, S., Hou, J., et al. 2015, AJ, arXiv:1505.01592